

Fingerprints of CuPt ordering in III-V semiconductor alloys: Valence-band splittings, band-gap reduction, and x-ray structure factors

Su-Huai Wei and Alex Zunger

National Renewable Energy Laboratory, Golden, Colorado 80401

(Received 21 November 1997)

Spontaneous CuPt ordering induces a band-gap reduction ΔE_g relative to the random alloy, a crystal field splitting Δ_{CF} at valence-band maximum, as well as an increase of spin-orbit splitting Δ_{SO} . We calculate these quantities for $\text{Al}_x\text{In}_{1-x}\text{P}$, $\text{Al}_x\text{In}_{1-x}\text{As}$, $\text{Ga}_x\text{In}_{1-x}\text{P}$, and $\text{Ga}_x\text{In}_{1-x}\text{As}$ using the local density approximation (LDA), as well as the more reliable LDA-corrected formalism. We further provide these values and the valence-band splittings ΔE_{12} (between $\bar{\Gamma}_{4,5v}$ and $\bar{\Gamma}_{6v}^{(1)}$) and ΔE_{13} (between $\bar{\Gamma}_{4,5v}$ and $\bar{\Gamma}_{6v}^{(2)}$) for these materials as a function of the degree η of long range order. In the absence of an independent measurement of η , experiment is currently able to deduce only the ratio $\Delta E_g/\Delta_{CF}$. Our LDA-corrected results for this quantity compare favorably with recent experiments for $\text{Ga}_x\text{In}_{1-x}\text{P}$ and $\text{Ga}_x\text{In}_{1-x}\text{As}$, but not for $\text{Al}_x\text{In}_{1-x}\text{P}$, where our calculation does not support the experimental assignment. The ‘‘optical LRO parameter η ’’ can be obtained by fitting our calculated $\Delta E_g(\eta)$ to the measured $\Delta E_g(\eta)$, and by expressing the measured $\Delta E_{12}(\eta)$ and $\Delta E_{13}(\eta)$ in terms of our calculated $\Delta_{CF}(\eta)$ and $\Delta_{SO}(\eta)$. We also provide the calculated x-ray structure factors for ordered alloys that can be used experimentally to deduce η independently. [S0163-1829(98)01715-9]

I. INTRODUCTION

Spontaneous CuPt-like ordering of isovalent $A_xB_{1-x}C$ semiconductor alloys has been widely observed in vapor phase growth of many III-V systems on (001) substrates.¹ The ordered phase consists of alternate cation monolayer planes $A_{x+\eta/2}B_{1-x-\eta/2}$ and $A_{x-\eta/2}B_{1-x+\eta/2}$ stacked along the [111] (or equivalent) directions, where $0 \leq \eta \leq 1$ is the long-range order (LRO) parameter. $\eta=1$ corresponds to the perfectly ordered phase, while $\eta=0$ corresponds to the disordered phase (Fig. 1). In *spontaneously* ordered semiconductor alloys, the degree of LRO η is not perfect. The degree of ordering depends on growth temperature, growth rates, III/V ratio, substrate misorientation, and doping.¹

When the zinc-blende (ZB) disordered alloy forms the long-range ordered CuPt superlattice, the unit cell is doubled, the Brillouin zone is reduced by half, and the point-group symmetry is changed from T_d to C_{3v} . These lead to a series of predicted and observed changes in material properties,¹⁻³ including the appearance of pyroelectricity,⁴ birefringence,^{5,6} modified NMR chemical shifts,^{7,8} new effective masses,^{9,10} new pressure deformation potentials,¹¹ polarization of spin,¹² and light,¹³⁻¹⁵ new Raman peaks^{16,17} and the appearance of a transition to high-energy folded-in states.^{18,19} Here, we focus on two other type of changes, namely, (i) new x-ray diffraction spots that appear at $\{\mathbf{G}_{ZB}\} + (1/2, 1/2, 1/2)$, where $\{\mathbf{G}_{ZB}\}$ are zinc-blende reciprocal lattice vectors, and (ii) the changes of electronic and optical properties near the band edge. These changes in the ordered alloy are due to the fact that in the ordered phase two zinc-blende \mathbf{k} points (and states associated with them) fold into a single \mathbf{k} point in the CuPt Brillouin zone. Those folded states that have the same superlattice symmetry can couple to each other. This coupling leads to energy-level shifts and to splitting of those states that were degenerate in the random alloy.^{14,19}

In the absence of spin-orbit coupling, the valence-band maximum (VBM) of the *random* alloy has $\bar{\Gamma}_{15v}$ symmetry and the conduction-band minimum (CBM) has $\bar{\Gamma}_{1c}$ symmetry. In the *ordered* material, the $\bar{\Gamma}_{15v}$ state splits into $\bar{\Gamma}_{3v}(\bar{\Gamma}_{15v})$ and $\bar{\Gamma}_{1v}(\bar{\Gamma}_{15v})$ (we denote ordered states with an overbar and indicate the zinc-blende parentage in parentheses) while the two lowest conduction states at $\bar{\Gamma}$ are $\bar{\Gamma}_{1c}(\bar{\Gamma}_{1c})$ and $\bar{\Gamma}_{1c}(L_{1c})$.

In the presence of spin-orbit coupling, the states near the VBM are

$$\begin{aligned} |1\rangle &= \bar{\Gamma}_{4,5v}, \\ |2\rangle &= \bar{\Gamma}_{6v}^{(1)}, \\ |3\rangle &= \bar{\Gamma}_{6v}^{(2)}. \end{aligned} \quad (1)$$

Here $|1\rangle$ is a pure ($j = \frac{3}{2}$, $m_j = \pm \frac{3}{2}$) state, while $|2\rangle$ and $|3\rangle$ are mixtures of ($j = \frac{3}{2}$, $m_j = \pm \frac{1}{2}$) and ($j = \frac{1}{2}$, $m_j = \pm \frac{1}{2}$) states. The conduction-band minimum is now $\bar{\Gamma}_{6c}$.

The optical fingerprints of ordering include the band-gap reduction relative to the random alloy:

$$\Delta E_g(\eta) = E_g(\eta) - E_g(0), \quad (2)$$

as well as the two valence-band splittings:

$$\Delta E_{12}(\eta) = E_1(\bar{\Gamma}_{4,5v}) - E_2(\bar{\Gamma}_{6v}^{(1)}), \quad (3)$$

$$\Delta E_{13}(\eta) = E_1(\bar{\Gamma}_{4,5v}) - E_3(\bar{\Gamma}_{6v}^{(2)}).$$

Using the quasicubic model^{13,20} the valence-band splittings at the top of the valence band for CuPt ordering are given by

$$\Delta E_{12}(\eta) = \frac{1}{2} [\Delta_{\text{SO}}(\eta) + \Delta_{\text{CF}}(\eta)] - \frac{1}{2} \left\{ [\Delta_{\text{SO}}(\eta) + \Delta_{\text{CF}}(\eta)]^2 - \frac{8}{3} \Delta_{\text{SO}}(\eta) \Delta_{\text{CF}}(\eta) \right\}^{1/2}, \quad (4)$$

$$\Delta E_{13}(\eta) = \frac{1}{2} [\Delta_{\text{SO}}(\eta) + \Delta_{\text{CF}}(\eta)] + \frac{1}{2} \left\{ [\Delta_{\text{SO}}(\eta) + \Delta_{\text{CF}}(\eta)]^2 - \frac{8}{3} \Delta_{\text{SO}}(\eta) \Delta_{\text{CF}}(\eta) \right\}^{1/2},$$

where $\Delta_{\text{SO}}(\eta)$ is the spin-orbit splitting and $\Delta_{\text{CF}}(\eta) = \bar{\Gamma}_{3v} - \bar{\Gamma}_{1v}$ is the ordering-induced crystal-field splitting in the absence of spin-orbit coupling. We found²¹ that physical properties $P(\eta)$ [e.g., the band gap $E_g(\eta)$, the crystal field splitting $\Delta_{\text{CF}}(\eta)$, the spin-orbit splitting $\Delta_{\text{SO}}(\eta)$, and the electron charge density $\rho(\mathbf{G}, \eta)$] of a partially ordered sample can be described by

$$P(x, \eta) = P(x, 0) + \eta^2 [P(X_{\sigma}, 1) - P(X_{\sigma}, 0)]. \quad (5)$$

This equation relates the property $P(x, \eta)$ at any degree of LRO η to (i) the corresponding properties $P(x, 0)$ of the perfectly random alloy at compositions x and (ii) the difference $P(X_{\sigma}, 1) - P(X_{\sigma}, 0)$ between the perfectly ordered structure and the perfectly random structure at composition $X_{\sigma} = 0.5$.

The quantities that are accessible experimentally are $\Delta E_{12}(\eta)$, $\Delta E_{13}(\eta)$, and $E_g(\eta)$ for partially ordered alloys and for random alloys. These values can be used to derive

$$\begin{aligned} \Delta_{\text{SO}}(\eta) - \Delta_{\text{SO}}(0) &= [\Delta_{\text{SO}}(1) - \Delta_{\text{SO}}(0)] \eta^2, \\ \Delta_{\text{CF}}(\eta) &= \Delta_{\text{CF}}(1) \eta^2, \\ \Delta E_g(\eta) &= \Delta E_g(1) \eta^2, \end{aligned} \quad (6)$$

using Eqs. (2), (4), and (5) [note that $\Delta_{\text{CF}}(0) = 0$]. Since (i) perfectly ordered ($\eta = 1$) samples are unavailable and (ii) the degree of LRO η of a given sample is not known independently, one cannot find $\Delta_{\text{SO}}(1)$, $\Delta_{\text{CF}}(1)$, and $\Delta E_g(1)$ by this fitting procedure.^{2,22} In fact, only the ratio

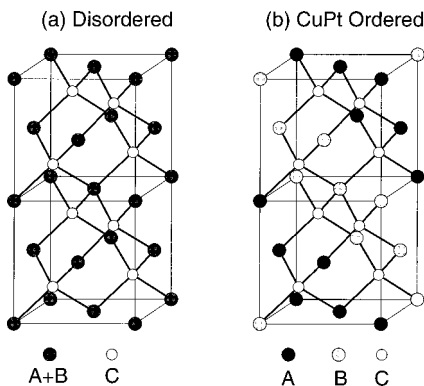


FIG. 1. Crystal structures of (a) disordered zinc-blende alloy and (b) fully CuPt ordered alloy.

$$\begin{aligned} \xi &= -\Delta E_g(1) / [\Delta_{\text{SO}}(1) - \Delta_{\text{SO}}(0)], \\ \zeta &= -\Delta E_g(1) / \Delta_{\text{CF}}(1) \end{aligned} \quad (7)$$

can be determined from experimental measurement of $\Delta E_{12}(\eta)$, $\Delta E_{13}(\eta)$, and $E_g(\eta)$. On the other hand, if $[\Delta_{\text{SO}}(1) - \Delta_{\text{SO}}(0)]$, $\Delta_{\text{CF}}(1)$, and $\Delta E_g(1)$ were known independently (e.g., from theoretical calculation), then experimental measurement of $\Delta E_{12}(\eta)$, $\Delta E_{13}(\eta)$, and $E_g(\eta)$ could be used to derive the ordering parameter η from the above equations. Similarly, if η is available independently (e.g., via x-ray diffraction or NMR measurement), measurements of $\Delta E_{12}(\eta)$, $\Delta E_{13}(\eta)$, and $E_g(\eta)$ could be used to deduce $\Delta_{\text{SO}}(1)$, $\Delta_{\text{CF}}(1)$, and $\Delta E_g(1)$ and compare with the theoretical results given here.

We have previously calculated the ordering-induced change²¹ $[\Delta_{\text{SO}}(1) - \Delta_{\text{SO}}(0)]$, $\Delta_{\text{CF}}(1)$, and $\Delta E_g(1)$, for ordered $\text{Ga}_{0.5}\text{In}_{0.5}\text{P}$ and $\text{Ga}_{0.5}\text{In}_{0.5}\text{As}$ alloys using the first-principles, local density approximation^{23,24} (LDA) as implemented by the self-consistent linearized augmented plane wave (LAPW) method.²⁵ In this paper, we (i) extend our calculation to include the ordered alloys of $\text{Al}_{0.5}\text{In}_{0.5}\text{P}$ and $\text{Al}_{0.5}\text{In}_{0.5}\text{As}$. We will point out the differences between the $\text{Al}_{0.5}\text{In}_{0.5}\text{X}$ ($\text{X} = \text{P}, \text{As}$) and the $\text{Ga}_{0.5}\text{In}_{0.5}\text{X}$ alloys. The LDA, however, includes some errors in the position of the conduction bands of the zinc-blende constituents²⁶ due to spurious self-interaction and due to the omission of explicit correlation.²⁴ We will thus (ii) correct the LDA errors and reevaluate the calculated parameters of ordered alloys. Furthermore, (iii) we calculated the x-ray structure factors of the perfectly ordered alloys. These data could be useful in analyzing experimental observations and in deriving the ordering parameters from measured experimental values of partially ordered samples.

II. LDA RESULTS

The band-structure calculations are performed using the fully relativistic, general potential LAPW method.²⁵ We used the Ceperley-Alder exchange correlation potential²³ as parametrized by Perdew and Zunger.²⁴ For the binary compounds the band structures are calculated at experimental²⁷ lattice constants. For the alloys the lattice constants are determined using the Vegard rule,²⁸ while the internal atomic relaxation are determined using the valence force field model.²⁹ We assume that the ordered alloy is coherent with the (lattice matched) (001) substrate, thus no [111] rhombohedral lattice vector distortion is allowed. The energy levels of the random alloys are obtained using the ‘‘special quasi-random structure’’ (SQS) approach.³⁰ We find that for these common-anion systems, the band gaps calculated using SQS are similar to those obtained from the average of the binary constituents deformed to the same lattice constants of the disordered alloy. The results of the LDA calculation are shown in the upper part of Table I. We find the following:

(i) Ordering induces large crystal-field splitting $\Delta_{\text{CF}}(1)$ and band-gap reductions $\Delta E_g(1)$ in all four alloy systems.

(ii) Comparing with $\text{Ga}_{0.5}\text{In}_{0.5}\text{X}$, the $\text{Al}_{0.5}\text{In}_{0.5}\text{X}$ alloys have larger crystal-field splitting. This is because the valence-band offsets between AlX/InX [~ 0.6 eV (Ref. 31)] is much larger than that for GaX/InX [~ 0.1 eV (Ref. 31)],

TABLE I. LDA and LDA-corrected values of ordering-induced changes in spin-orbit splitting [$\Delta_{\text{SO}}(1) - \Delta_{\text{SO}}(0)$], crystal-field splitting $\Delta_{\text{CF}}(1)$, band-gap reduction $\Delta E_g(1)$ (in eV), and the ratio $\zeta = -\Delta E_g(1)/\Delta_{\text{CF}}(1)$ for the four III-V alloys.

	Al _{0.5} In _{0.5} P	Al _{0.5} In _{0.5} As	Ga _{0.5} In _{0.5} P	Ga _{0.5} In _{0.5} As
	LDA values			
$[\Delta_{\text{SO}}(1) - \Delta_{\text{SO}}(0)]$	0.02	0.01	0.01	0.00
$\Delta_{\text{CF}}(1)$	0.26	0.24	0.20	0.10
$\Delta E_g(1)$	-0.17	-0.14	-0.32	-0.30
ζ	0.65	0.58	1.60	3.00
	LDA corrected values			
$[\Delta_{\text{SO}}(1) - \Delta_{\text{SO}}(0)]$	0.02	0.01	0.01	0.00
$\Delta_{\text{CF}}(1)$	0.24	0.21	0.16	0.13
$\Delta E_g(1)$	-0.27	-0.18	-0.43	-0.25
ζ	1.13	0.86	2.69	1.92

thus, there is a larger perturbation in the valence band of Al_{0.5}In_{0.5}X than in Ga_{0.5}In_{0.5}X.

(iii) The band-gap reduction $\Delta E_g(1)$ is smaller in Al_{0.5}In_{0.5}X than in Ga_{0.5}In_{0.5}X. This can be understood by noticing that (1) the LDA atomic s orbital energies of Al, Ga, and In are nonmonotonic, namely, -7.9 , -9.3 , and -8.6 eV, respectively, and (2) atomic relaxation in lattice mismatch common-anion alloys tends to shift the charge from the long bond (In-X) to the short bonds (Ga-X in Ga_{0.5}In_{0.5}X and Al-X in Al_{0.5}In_{0.5}X).³² Consequently, the band-gap reduction due to atomic relaxation is larger in Ga_{0.5}In_{0.5}X (since Ga receives charge, and its s is deeper in energy than In), but smaller in Al_{0.5}In_{0.5}X (since Al receives charge, and its s is shallower in energy than In).

(iv) Relative to the random alloy, the VBM wave function of the ordered compounds is more localized on the cation having larger atomic number.³³ Thus, $[\Delta_{\text{SO}}(1) - \Delta_{\text{SO}}(0)] > 0$. However, for common-anion systems Δ_{SO} of the two binary constituents are similar, thus the ordering-induced increase $[\Delta_{\text{SO}}(1) - \Delta_{\text{SO}}(0)]$ is rather small (0.00–0.02 eV). The increase is slightly greater for Al_{0.5}In_{0.5}X than for Ga_{0.5}In_{0.5}X, because of the larger atomic number difference between Al and In.

III. LDA CORRECTIONS

It is well known²⁴ that the LDA underestimates the band gap. This is seen in Table II and Table III where our LDA

TABLE II. Comparison between the calculated fully relativistic energy levels (in eV) and the available experimental values (Ref. 27) for AIP, GaP, and InP. The calculated results are obtained at experimental lattice constants ($a = 5.467$, 5.451 , and 5.869 Å, respectively) using LDA, LDA+correction (LDA+C), and quasiparticle (QP) methods (Ref. 26). The energy zero is at the VBM (Γ_{8v}).

State	AIP				GaP				InP			
	LDA	LDA+C	Expt.	QP	LDA	LDA+C	Expt.	QP	LDA	LDA+C	Expt.	QP
X_{6c}	1.43	2.47	2.51	2.59	1.47	2.53	2.35	2.55	1.57	2.47	2.38	2.58
L_{6c}	2.62	3.63	3.57	3.90	1.42	2.53	2.71	2.67	1.22	2.01	1.99	2.28
Γ_{6c}	3.06	4.42		4.38	1.50	2.86	2.86	2.85	0.37	1.40	1.46	1.44
Γ_{8v}	0.00	0.00	0.00	0.00	0.00	0.00	0.00	0.00	0.00	0.00	0.00	0.00
Γ_{7v}	-0.06	-0.06			-0.09	-0.09	-0.08		-0.11	-0.11	-0.11	
$L_{4,5v}$	-0.77	-0.78	-0.8	-0.85	-1.17	-1.16	-1.2	-1.16	-0.99	-0.98	-1.23	-1.02
X_{7v}	-2.13	-2.06	-2.27	-2.31	-2.80	-2.70	-2.7	-2.78	-2.38	-2.31	-2.24	-2.38

gaps of binary zinc-blende compounds are compared with experiment.²⁷ Since the level repulsion between the states depends on the energy separations, these LDA errors will affect the calculated crystal-field splitting Δ_{CF} and the band-gap reduction ΔE_g (the effect on Δ_{SO} is, however, negligible).

Several methods have been proposed to correct these LDA errors, e.g., calculating the quasiparticle (QP) energies.²⁶ In this study, we use the fact that the LDA errors $e_{n,k}^{\text{LDA}} - \epsilon_{n,k}^{\text{expt}}$ for band n and wave vector k are known for the binary constituents (Table II and Table III). We thus design a cure for LDA that reproduce, via a fit, the state-dependent errors in the *zinc-blende binaries*, and then use this approach for the pseudobinary alloys $A_{1-x}B_xC$, assuming that the LDA error does not change with alloying. Instead of shifting energy bands rigidly, we use a self-consistent approach with *atom-dependent LDA corrections*. Specifically, we add to the LDA calculations external potentials³⁴ inside the muffin-tin spheres centered at each atomic site α :

$$V_{\text{ext}}^{\alpha}(r) = \bar{V}^{\alpha} + V_0^{\alpha} \left(\frac{r_0^{\alpha}}{r} \right) e^{-(r/r_0^{\alpha})^2}, \quad (8)$$

and performed the calculation self-consistently. The parameters \bar{V}^{α} , V_0^{α} , and r_0^{α} in Eq. (8) are fitted to the available experimental energy levels²⁷ (Table II and Table III) and to the quasiparticle energies calculated by Zhu and Louie²⁶ for the *binary constituents*. In order to improve the fit, empty spheres centered at tetrahedral sites³⁴ are also used. The muffin-tin radii are 2.23, 2.23, 2.50, 2.05, 2.05, and 2.05 a.u. for Al, Ga, In, P, As, and empty spheres, respectively. The fitting parameters are given in Table IV. The fitted results for the energy levels are given in Table II for the phosphides and in Table III for the arsenides. The same parameters given in Table IV are used in the calculation for the pseudobinary alloys. Due to the simple functional form of Eq. (8) and the errors in the fitting, we estimate that the uncertainty in the calculated LDA-corrected Δ_{CF} is about 0.02 eV and is about 0.04 eV for ΔE_g .

The lower part of Table I shows the calculated ordering-induced change $[\Delta_{\text{SO}}(1) - \Delta_{\text{SO}}(0)]$, $\Delta_{\text{CF}}(1)$, and $\Delta E_g(1)$ after the LDA correction. Comparing the results with the LDA predictions, we see that the general trends discussed above still hold. However, after the LDA correction we find the following:

TABLE III. Comparison between the calculated fully relativistic energy levels (in eV) and the available experimental values (Ref. 27) for AlAs, GaAs, and InAs. The calculated results are obtained at experimental lattice constants ($a=5.660, 5.653, \text{ and } 6.058 \text{ \AA}$, respectively) using LDA, LDA+correction (LDA+C), and quasiparticle (QP) method (Ref. 26). The energy zero is at the VBM (Γ_{8v}).

State	AlAs				GaAs				InAs			
	LDA	LDA+C	Expt.	QP	LDA	LDA+C	Expt.	QP	LDA	LDA+C	Expt.	QP
X_{6c}	1.25	2.23	2.37	2.14	1.23	2.22	1.98	2.01	1.31	2.16	2.34	2.01
L_{6c}	1.92	2.90	2.81	2.91	0.68	1.75	1.81	1.64	0.61	1.39	1.71	1.43
Γ_{6c}	1.75	3.05	3.13	2.88	0.09	1.43	1.52	1.22	-0.64	0.36	0.42	0.31
Γ_{8v}	0.00	0.00	0.00	0.00	0.00	0.00	0.00	0.00	0.00	0.00	0.00	0.00
Γ_{7v}	-0.30	-0.30	-0.28		-0.35	-0.34	-0.34		-0.37	-0.36	-0.37	
$L_{4,5v}$	-0.84	-0.85	-0.88	-0.99	-1.20	-1.19	-1.30	-1.28	-1.02	-1.01	-0.9	-1.13
X_{7v}	-2.21	-2.14	-2.38	-2.44	-2.82	-2.73	-2.96	-2.87	-2.49	-2.42	-2.4	-2.49

(i) $\Delta_{CF}(1)$ is reduced for $\text{Al}_{0.5}\text{In}_{0.5}\text{P}$, $\text{Al}_{0.5}\text{In}_{0.5}\text{As}$, and $\text{Ga}_{0.5}\text{In}_{0.5}\text{P}$, but increased for $\text{Ga}_{0.5}\text{In}_{0.5}\text{As}$. This can be understood by noticing that the LDA correction shifts the $\bar{\Gamma}_{1c}(\Gamma_{1c})$ upwards. For $\text{Al}_{0.5}\text{In}_{0.5}\text{P}$, $\text{Al}_{0.5}\text{In}_{0.5}\text{As}$, and $\text{Ga}_{0.5}\text{In}_{0.5}\text{P}$ alloys, where LDA calculations already give positive band gaps, the upward shift of $\bar{\Gamma}_{1c}(\Gamma_{1c})$ reduces the repulsion between the $\bar{\Gamma}_{1c}(\Gamma_{1c})$ and $\bar{\Gamma}_{1v}(\Gamma_{15v})$, thus reducing the crystal-field splitting. On the other hand, LDA calculation gives a negative band gap for $\text{Ga}_{0.5}\text{In}_{0.5}\text{As}$, i.e., $\bar{\Gamma}_{1c}^{\text{LDA}}(\Gamma_{1c})$ is below $\bar{\Gamma}_{1v}^{\text{LDA}}(\Gamma_{15v})$. After the LDA correction, the order is reversed, thus, the level repulsion *increases* Δ_{CF} .

(ii) The band-gap reduction $\Delta E_g(1)$ is increased for $\text{Al}_{0.5}\text{In}_{0.5}\text{P}$, $\text{Al}_{0.5}\text{In}_{0.5}\text{As}$, and $\text{Ga}_{0.5}\text{In}_{0.5}\text{P}$ alloys, but decreased for $\text{Ga}_{0.5}\text{In}_{0.5}\text{As}$. Again, this reflects the change in level repulsions. For example, in $\text{Ga}_{0.5}\text{In}_{0.5}\text{P}$, the average Γ_{1c} and L_{1c} energy-level separation is reduced from 0.38 to 0.14 eV after the LDA correction. This increases the level repulsion between the Γ_{1c} and L_{1c} derived states and leads to a larger $\Delta E_g(1)$ after the LDA correction.

(iii) Due to the effects discussed in (i) and (ii), after the LDA correction the ratio of band-gap reduction to crystal-field splitting ζ [Eq. (7)] is increased for $\text{Al}_{0.5}\text{In}_{0.5}\text{P}$, $\text{Al}_{0.5}\text{In}_{0.5}\text{As}$, and $\text{Ga}_{0.5}\text{In}_{0.5}\text{P}$ alloys, but decreased for $\text{Ga}_{0.5}\text{In}_{0.5}\text{As}$.

IV. COMPARISON WITH EXPERIMENT

(1) GaInP_2 : Recently, Fluegel *et al.*³⁵ measured the ratio ζ using a pump-probe exciton absorption/bleaching method. They find that for GaInP_2 , $\zeta = 2.66 \pm 0.15$. This value is considerably larger than our LDA-calculated values of $\zeta = 1.60$

TABLE IV. Fitted parameters \bar{V} , V_0 (in Ry), and r_0 (in a.u.) [see Eq. (3)] for the LDA corrections.

Atom	\bar{V}	V_0	r_0
P	0.00	80	0.025
As	0.00	80	0.025
Al	0.00	360	0.025
Ga	0.00	280	0.025
In	0.00	200	0.025
Empty sphere	0.36	100	0.025

(Table I) but is very close to our LDA-corrected value of $\zeta = 2.69$.

(2) GaInAs_2 : Using low-temperature absorption and photoluminescence, Wirth *et al.*³⁶ measured the band-gap reduction and valence-band splitting of partially ordered $\text{Ga}_x\text{In}_{1-x}\text{As}$ alloys. They derived from their experimental data that for GaInAs_2 $\zeta = 1.8 \pm 0.4$. This value is close to our LDA-corrected value $\zeta = 1.92$.

(3) AlInP_2 : Using dark-field spectroscopy, Schubert *et al.*³⁷ have measured ζ for $\text{Al}_x\text{In}_{1-x}\text{P}$ alloy and find that the ratio is only 0.14, much smaller than our LDA-corrected value of 1.13. Further, they show that in some of the samples the measured valence-band splitting ΔE_{12} is larger than 0.08 eV, while our calculations show that even for perfectly ordered $\text{Al}_{0.5}\text{In}_{0.5}\text{P}$, ΔE_{12} is less than 0.07 eV. Thus, we believe that their ΔE_{12} is overestimated. This also contributed to the small ζ derived by them.

V. X-RAY STRUCTURE FACTORS

To aid in the experimental identification of the ordered CuPt-like crystal structures and the determination of the de-

TABLE V. Calculated structure factors $|\rho(\mathbf{G})|$ of fully CuPt ordered AlInP_2 , AlInAs_2 , GaInP_2 , and GaInAs_2 (in electrons per atom). Since the charge density is a real number $|\rho(-\mathbf{G})| = |\rho(\mathbf{G})|$. Furthermore, for \mathbf{G} vectors in the same star $[(x,y,z)$ and its cyclical permutations] the structural factors are the same. Here, the reciprocal lattice vector \mathbf{G} is in units of $2\pi/a$, where a is the cubic lattice constant. An asterisk next to a \mathbf{G} vector indicates that it is a superstructure spot.

\mathbf{G}	AlInP_2	AlInAs_2	GaInP_2	GaInAs_2
0,0,0	23.00	32.00	27.50	36.50
$*\frac{1}{2}, \frac{1}{2}, \frac{1}{2}$	8.26	7.79	3.83	3.39
$*\frac{1}{2}, \frac{1}{2}, \frac{3}{2}$	8.02	7.91	3.83	3.70
1,1,1	14.43	19.53	18.28	22.55
1,1,1	14.20	19.11	18.12	22.23
0,0,2	7.16	0.94	11.21	3.17
$*\frac{1}{2}, \frac{3}{2}, \frac{3}{2}$	8.30	9.25	4.34	5.33
$*\frac{1}{2}, \frac{1}{2}, \frac{5}{2}$	8.16	9.52	4.51	6.00
$*\frac{3}{2}, \frac{3}{2}, \frac{3}{2}$	6.48	5.74	3.01	3.26
2,0,2	15.94	23.73	19.58	27.43
2,2,0	15.77	23.36	19.40	27.04

gree of ordering, we have calculated the static x-ray structure factors $\rho(\mathbf{G})$ of the fully ordered AlInP₂, AlInAs₂, GaInP₂, and GaInAs₂. The structure factors $\rho(\mathbf{G})$ are the Fourier transform of the electron charge density $\rho(\mathbf{r})$, i.e.,

$$\rho(\mathbf{G}) = \frac{1}{\Omega} \int_{\Omega} \rho(\mathbf{r}) e^{i\mathbf{G} \cdot \mathbf{r}} d\mathbf{r}. \quad (9)$$

Here \mathbf{G} is the reciprocal lattice vector and Ω is the unit cell volume. The diffraction intensity I is proportional to $|\rho(\mathbf{G})|^2$.

Our calculated results are shown in Table V. We find that (i) the structure factors for the ordered alloy taken at the ZB allowed $\{\mathbf{G}_{\text{ZB}}\}$ are very similar to those of the random alloys (not shown), except for some small splittings due to the lower symmetry of the ordered alloy. However, (ii) new structure factors appear at $\{\mathbf{G}_{\text{ZB}}\} + (1/2, 1/2, 1/2)$ in the ordered alloy that do not exist in the perfectly random alloy. Observation of $\rho(\mathbf{G})$ at these superstructure spots (marked with an asterisk in Table V) would be one of the strongest indications of the existence of the ordered phase. Since $\rho(\mathbf{G})$ for these new structure factors is proportional to η^2 , accurate measurement of the intensity of the diffraction spectrum $I(\mathbf{G}, \eta)$ can, in principle, be used to derive the degree of order η by comparing it with the calculated values for perfectly ordered systems (Table V).

In an actual experimental measurement at finite temperature, the measured intensity is reduced by the thermal vibration of the lattice. The dynamic (temperature) effect is often approximated by the Debye-Waller factors.³⁸ In this approximation the relation between the measured dynamic structure factor $\rho_{\text{expt}}(\mathbf{G}, \eta)$ and the calculated static structure factor $\rho_{\text{calc}}(\mathbf{G}, \eta)$ is

$$\rho_{\text{expt}}(\mathbf{G}, \eta) = \rho_{\text{calc}}(\mathbf{G}, \eta) e^{-B(T)G^2}, \quad (10)$$

where $B(T)$ is a temperature-dependent constant. Since $\rho(\mathbf{G}_{\text{ZB}}, \eta)$ is essentially ordering independent for the zincblende allowed \mathbf{G}_{ZB} vectors, measuring $\rho_{\text{expt}}(\mathbf{G}_{\text{ZB}})$ can be used to derive the value B from Eq. (10) and Table V. This B can in turn be used in Eq. (10) to calculate $\rho_{\text{calc}}(\mathbf{G}, \eta)$ from measured $\rho_{\text{expt}}(\mathbf{G})$ for the superstructure spots. Finally, the obtained $\rho_{\text{calc}}(\mathbf{G}, \eta)$ can be used to derive the ordering parameters η using Eq. (5) and the values given in Table V. Experimental testing of our predictions are called for.

VI. SUMMARY

We have calculated the ordering-induced changes in the crystal-field splitting, spin-orbit splitting, and band gap relative to the random alloy for Al_{0.5}In_{0.5}P, Al_{0.5}In_{0.5}As, Ga_{0.5}In_{0.5}P, and Ga_{0.5}In_{0.5}As alloy using the local density approximation, as well as the more reliable LDA-corrected formalism. We provide these values for these materials as a function of the degree η of long-range order. Our LDA-corrected results compare favorably with recent experiments for Ga_xIn_{1-x}P and Ga_xIn_{1-x}As, but not for Al_xIn_{1-x}P, where our calculation does not support the experimental assignment. We also calculated x-ray structure factors for these ordered alloys, which can be used experimentally to deduce the ordering parameter η .

ACKNOWLEDGMENTS

This work was supported in part by the U.S. Department of Energy, OER-BES, Grant No. DE-AC36-83-CH10093.

¹For a recent review on spontaneous ordering in semiconductor alloys, see A. Zunger and S. Mahajan, in *Handbook of Semiconductors*, 2nd ed., edited by S. Mahajan (Elsevier, Amsterdam, 1994), Vol. 3, p. 1399, and references therein.
²S.-H. Wei, A. Franceschetti, and A. Zunger, in *Optoelectronic Materials-Ordering, Composition Modulation, and Self-Assembled Structures*, edited by E. D. Jones, A. Mascarenhas, and P. Petroff, MRS Symposia Proceedings No. 417 (Materials Research Society, Pittsburgh, 1996), p. 3.
³A. Zunger, MRS Bull. **22**, 20 (1997).
⁴R. G. Alonso, A. Mascarenhas, G. S. Horner, K. A. Bertness, S. R. Kurtz, and J. M. Olson, Phys. Rev. B **48**, 11 833 (1993).
⁵R. Wirth, A. Moritz, C. Geng, F. Scholz, and A. Hangleiter, Phys. Rev. B **55**, 1730 (1997).
⁶Y. Zhang, B. Fluegel, A. Mascarenhas, J. F. Geisz, J. M. Olson, F. Alsina, and A. Duda, Solid State Commun. **104**, 577 (1997).
⁷D. Mao, P. C. Tayler, S. R. Kurtz, M. C. Wu, and W. A. Harrison, Phys. Rev. Lett. **76**, 4769 (1996).
⁸S.-H. Wei and A. Zunger, J. Phys. Chem. **107**, 1931 (1997).
⁹A. Franceschetti, S.-H. Wei, and A. Zunger, Phys. Rev. B **52**, 13 992 (1995).
¹⁰Y. Zhang and A. Mascarenhas, Phys. Rev. B **51**, 13 162 (1995); P. Ernst, Y. Zhang, F. A. J. M. Driessen, A. Mascarenhas, E. D. Jones, C. Geng, F. Scholz, and H. Schweizer, J. Appl. Phys. **81**, 2814 (1997).

¹¹A. Franceschetti and A. Zunger, Appl. Phys. Lett. **65**, 2990 (1994).
¹²S.-H. Wei and A. Zunger, Appl. Phys. Lett. **64**, 1676 (1994).
¹³A. Mascarenhas, S. Kurtz, A. Kibbler, and J. M. Olson, Phys. Rev. Lett. **63**, 2108 (1989).
¹⁴S.-H. Wei and A. Zunger, Phys. Rev. B **49**, 14 337 (1994); **51**, 14 110 (1995).
¹⁵J. S. Luo, J. M. Olson, K. A. Bertness, M. E. Raikh, and E. V. Tsiper, J. Vac. Sci. Technol. B **12**, 2552 (1994).
¹⁶F. Alsina, N. Mestres, J. Pascual, C. Geng, P. Ernst, and F. Scholz, Phys. Rev. B **53**, 12 994 (1996); H. M. Cheong, A. Mascarenhas, P. Ernst, and C. Geng, Phys. Rev. B **56**, 1882 (1997).
¹⁷V. Ozolins and A. Zunger (unpublished).
¹⁸F. Alsina, M. Garriga, M. I. Alonso, J. Pascual, and R. W. Glew, in *Proceedings of the 22nd International Conference on the Physics of Semiconductors, Vancouver, Canada*, edited by D. J. Lockwood (World Scientific, Singapore, 1994), p. 253.
¹⁹S.-H. Wei, A. Franceschetti, and A. Zunger, Phys. Rev. B **51**, 13 097 (1994).
²⁰J. J. Hopfield, J. Phys. Chem. Solids **15**, 97 (1960).
²¹S.-H. Wei, D. B. Laks, and A. Zunger, Appl. Phys. Lett. **62**, 1937 (1993).
²²P. Ernst, C. Geng, F. Scholz, and H. Schweizer, Y. Zhang, A.

- Mascarenhas, Appl. Phys. Lett. **67**, 2347 (1995).
- ²³D. M. Ceperly and B. J. Alder, Phys. Rev. Lett. **45**, 566 (1980).
- ²⁴J. P. Perdew and A. Zunger, Phys. Rev. B **23**, 5048 (1981).
- ²⁵S.-H. Wei and H. Krakauer, Phys. Rev. Lett. **55**, 1200 (1985), and references therein.
- ²⁶X. Zhu and S. G. Louie, Phys. Rev. B **43**, 14 142 (1991).
- ²⁷*Semiconductors. Physics of Group IV Elements and III-V Compounds*, edited by O. Madelung, M. Schulz, and H. Weiss, Landolt-Börnstein, New Series, Group III, Vol. 17, Pt. a (Springer-Verlag, Berlin, 1982); *Intrinsic Properties of Group IV Elements and II-V, II-VI, and I-VII Compounds*, edited by O. Madelung, M. Schulz, and H. Weiss, Landolt-Börnstein, New Series, Group III, Vol. 22, Pt. a (Springer, Berlin, 1987).
- ²⁸L. Vegard, Z. Phys. **5**, 17 (1921).
- ²⁹J. L. Martins and A. Zunger, Phys. Rev. B **30**, 6217 (1984).
- ³⁰A. Zunger, S.-H. Wei, L. G. Ferreira, and J. E. Bernard, Phys. Rev. Lett. **65**, 353 (1990); S.-H. Wei, L. G. Ferreira, J. E. Bernard, and A. Zunger, Phys. Rev. B **42**, 9622 (1990).
- ³¹S.-H. Wei and A. Zunger (unpublished).
- ³²S.-H. Wei and A. Zunger, Phys. Rev. Lett. **76**, 664 (1996).
- ³³S.-H. Wei and A. Zunger, Phys. Rev. B **39**, 6279 (1989).
- ³⁴N. E. Christensen, Phys. Rev. B **30**, 5753 (1984).
- ³⁵B. Fluegel, Y. Zhang, H. M. Cheong, A. Mascarenhas, J. F. Geisz, J. M. Olson, and A. Duda, Phys. Rev. B **55**, 13 647 (1997).
- ³⁶R. Wirth, H. Seitz, M. Geiger, F. Scholz, A. Hangleiter, A. Muhe, and F. Phillipp, Appl. Phys. Lett. **71**, 2127 (1997).
- ³⁷M. Schubert, B. Rheinlander, E. Franke, I. Pietzonka, J. Skriniarova, and V. Gottschalch, Phys. Rev. B **54**, 17 616 (1997).
- ³⁸Z. W. Lu, A. Zunger, and M. Deutsch, Phys. Rev. B **47**, 9385 (1993).